PHILOSOPHICAL TRANSACTIONS OF THE ROYAL SOCIETY A MATHEMATICAL, PHYSICAL & ENGINEERING SCIENCES

Physics and control of wall turbulence for drag reduction

John Kim

Phil. Trans. R. Soc. A 2011 **369**, 1396-1411
doi: 10.1098/rsta.2010.0360

PHILOSOPHICAL TRANSACTIONS OF THE ROYAL SOCIETY A

Phil. Trans. R. Soc. A (2011) **369**, 1396–1411
doi:10.1098/rsta.2010.0360

Physics and control of wall turbulence for drag reduction

By John Kim*

Department of Mechanical and Aerospace Engineering, University of California, Los Angeles, CA 90095-1597, USA

Turbulence physics responsible for high skin-friction drag in turbulent boundary layers is first reviewed. A self-sustaining process of near-wall turbulence structures is then discussed from the perspective of controlling this process for the purpose of skin-friction drag reduction. After recognizing that key parts of this self-sustaining process are linear, a linear systems approach to boundary-layer control is discussed. It is shown that singular-value decomposition analysis of the linear system allows us to examine different approaches to boundary-layer control without carrying out the expensive nonlinear simulations. Results from the linear analysis are consistent with those observed in full nonlinear simulations, thus demonstrating the validity of the linear analysis. Finally, fundamental performance limit expected of optimal control input is discussed.

Keywords: turbulent boundary layer; drag reduction; flow control

1. Introduction

Successful flow control can lead to significant financial benefits. Worldwide, ocean shipping, for example, consumes about 2.1 billion barrels of oil per year (per 2003 figures). If we could save 30 per cent of the fuel consumption by a flow-control scheme that reduces the skin-friction drag in turbulent boundary layers (TBLs), it would result in a saving of $38 billion per year (based on $60 per barrel) for shipping industries. The impact on the reduction of emissions of pollutants would be equally impressive. A similar argument can be made for airline and trucking industries, which consume, respectively, 1.5 billion barrels and 1.2 billion barrels of oil per year.

The control of TBLs requires a thorough understanding of the underlying physics of TBLs, and an efficient control algorithm, both of which have been less than satisfactory despite the great interest they have garnered over the years. Great strides on both fronts have been made recently through the advancement in computational fluid dynamics and control theories. The availability of accurate time history of full three-dimensional velocity and pressure fields has led to improved understanding of the underlying physics of turbulent flows. Numerical simulations have resolved many existing controversies by putting together bits of information collected by different experimental techniques. Numerical

*jkim@seas.ucla.edu

One contribution of 15 to a Theme Issue ‘Flow-control approaches to drag reduction in aerodynamics: progress and prospects’.

simulations have also been extremely useful in testing various hypotheses by conducting cleverly designed numerical experiments, in which modified Navier–Stokes equations were solved in order to examine the role of certain turbulence mechanisms (e.g. [1,2]). On the control front, new approaches to controller design that are significantly different from existing approaches have emerged. In contrast to most existing approaches, which were largely based on the investigator's physical insight into the flow, new approaches incorporate modern control theories into the controller design [3]. Some of these approaches explicitly exploit certain linear mechanisms present in TBLs, and their success suggests the importance of linear mechanisms in turbulent (and hence, nonlinear) flows.

The objective of this paper is to present a unified overview of the author's work[1] on turbulence control aimed at achieving viscous drag reduction in TBLs. I shall first discuss the underlying physics of turbulence that is responsible for high skin-friction drag in TBLs, and then discuss a linear systems approach to boundary-layer control. This linear systems approach is based on the recognition that much of the underlying physics of turbulence responsible for large skin-friction drag in TBLs is a linear process. It is worth mentioning that, in spite of the apparent differences in the outer region, near-wall turbulence structures as well as near-wall turbulence statistics are almost identical for turbulent channels and TBLs, especially from the perspective of control of near-wall turbulence for the purpose of drag reduction. Since the major concern of this paper is related to near-wall turbulence, no effort is made to differentiate between the two flows, and the term turbulent boundary layers (TBLs) is used throughout this paper.[2]

In this paper, x, y and z denote the streamwise, wall-normal and spanwise directions, respectively. The velocities are u, v and w in the x, y and z directions, respectively. An overhat, as in $\hat{u}$, denotes a Fourier-transformed quantity. The superscript $+$ indicates a non-dimensional quantity scaled by the wall variables: e.g. $y^+ = yu_\tau/\nu$, where ν is the kinematic viscosity, $u_\tau = \sqrt{\nu\, \mathrm{d}U/\mathrm{d}y|_\mathrm{w}}$ is the wall-shear velocity, and $\mathrm{d}U/\mathrm{d}y|_\mathrm{w}$ is the mean velocity gradient at the wall.

2. Physics of near-wall turbulence

The discovery of well-organized turbulence structures and the recognition that these structures play important roles in the wall-layer dynamics are among the major advances in turbulent boundary-layer research during the past several decades. The ubiquitous structural features in the near-wall region of TBLs are low- and high-speed 'streaks', which consist mostly of a spanwise modulation of the streamwise velocity. These streaks are created by streamwise vortices, which are roughly aligned in the streamwise direction. It has now been recognized, in large part due to numerical investigations, that streamwise vortices are also responsible for the high skin-friction drag. These vortices are primarily found in the buffer layer ($y^+ = 10$–50), with their typical diameter of the order of $d^+ = 20$–50 [4]. There is strong evidence that most high skin-friction regions in turbulent boundary layers are induced by nearby streamwise vortices. A common feature of all drag-reduced flows, regardless of how the drag was reduced (e.g.

[1]This overview is limited to the author's previous work, and some contents in this paper are directly from the author's prior publications and public presentations.

[2]Section 5 is an exception, which, as presented, applies only to fully developed channel flows.

polymer in [5,6], micro-bubble in [7], and hydrophobic surface in [8], to name but a few), is weakened near-wall streamwise vortices, as illustrated in figure 1. The strength of streaks is also significantly reduced and their average spanwise spacing is increased.

Streamwise vortices are formed and maintained autonomously (i.e. independent of the outer layer) by a self-sustaining process, which involves wall-layer streaks and instabilities associated with them [1,9–12]. There are some differences in the details of the self-sustaining (or regeneration) process (see the references mentioned above for further details), but it is generally accepted that this process is independent of (at least in the first order) the outer part of the boundary layer, and that the presence of a wall itself does not play a role in the process other than setting up the mean shear through the no-slip boundary condition on the streamwise velocity. A generally accepted regeneration cycle, with the exception of some minor details, is shown in figure 2.[3] One can start from any place in the cycle, but let us start from the first leg of the cycle, which involves interactions between streamwise vortices and mean shear. Streamwise vortices (sometimes referred to as streamwise rolls) primarily consist of the wall-normal and spanwise velocities, independent of the streamwise direction, i.e. $v(z)$ and $w(z)$, respectively. These vortices create streaks, i.e. $u(z)$, through interaction with the mean shear, $\mathrm{d}U/\mathrm{d}y$. This process is sometimes referred to as lift-up (of low-momentum fluid). It is also related to the so-called transient growth of disturbances—streamwise disturbances in particular—due to the non-normality (or non-self-adjointness) of the linearized Navier–Stokes equations. The streaks can also be identified by the presence of strong wall-normal vorticity, $\omega_y(z)$, at both edges of the streaks. Note that this lift-up process (first leg in the regeneration cycle) is linear. The strength of streaks can grow indefinitely as long as the strength of the streamwise vortices and the mean shear are maintained. However, these streamwise-independent vortices will ultimately decay unless they are strengthened through a nonlinear mechanism involving streamwise-dependent disturbances, as shown in the third leg of the regeneration cycle. Hamilton *et al.* [9] presented a vortex formation mechanism, in which an advection term, $v(\partial\omega_x/\partial y)$, played a dominant role, whereas Schoppa & Hussain [10] showed that a vortex stretching term, $\omega_x(\partial u/\partial x)$, was responsible for creating streamwise vortices. It is worth mentioning that both mechanisms do not require the presence of existing vortices for vortex formation, in contrast to other generation mechanisms, which require strong pre-existing vortices (e.g. [13,14]). Note also that both mechanisms involve streamwise-dependent disturbances, and that they are nonlinear.

Streaks created by the linear mechanism (first leg in the regeneration cycle) are unstable to small disturbances, i.e. linearly unstable. They are unstable to the classical normal-mode type disturbances, i.e. there are unstable eigenmodes associated with spanwise-varying mean velocity profiles, $U(y,z)$ [9,12]. In addition to this normal-mode instability, Schoppa & Hussain [10] showed that streaks are also subject to non-normal-mode instability (referred to as streak

[3]The schematic illustrates a simplified model consisting of key elements necessary to maintain near-wall turbulence. Actual turbulent flows may contain more complex structures. For example, the x-independent streamwise vortex in this model can be a part of inclined quasi-streamwise vortical structures, which are approximately parallel to the wall in the wall region.

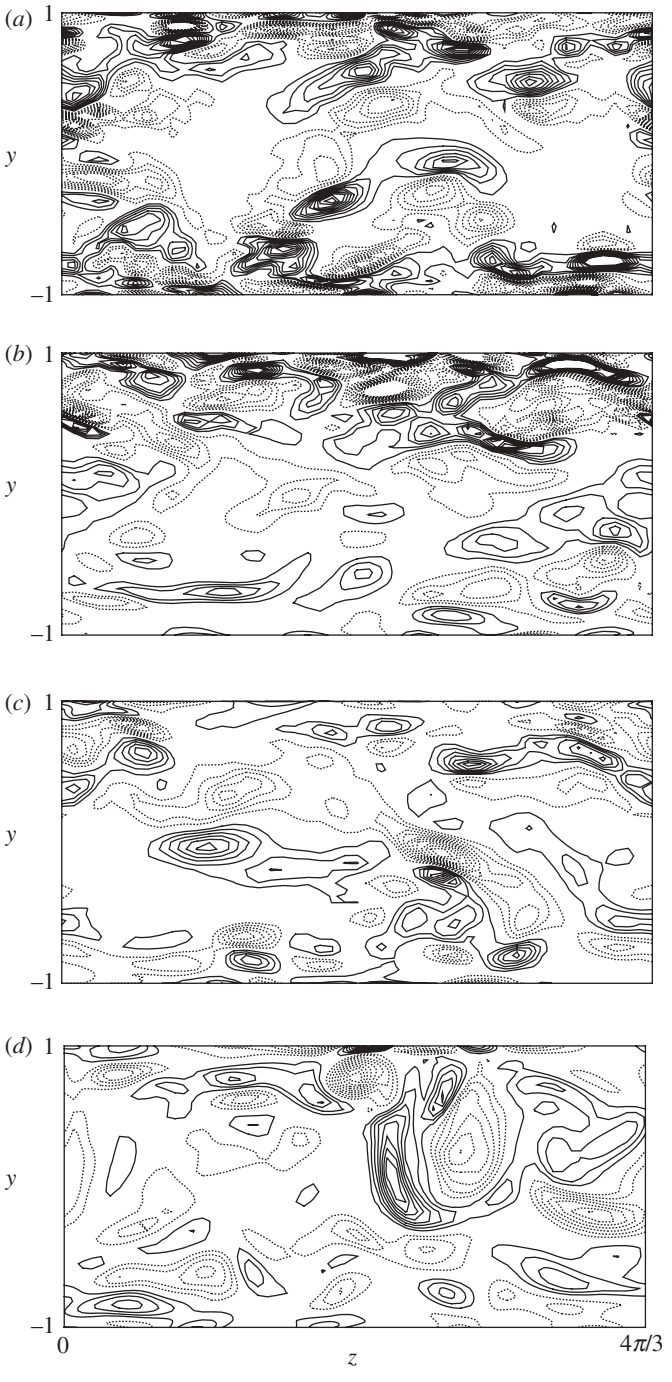

Figure 1. Contours of streamwise vorticity in the y–z plane: (a) regular channel; (b) channel with an LQR controller on the bottom wall (T. Min 2005, unpublished data); (c) channel with a hydrophobic surface on both walls [8]; and (d) channel with a polymer [6]. Contour levels are from −1 to 1 in increments of 0.1.

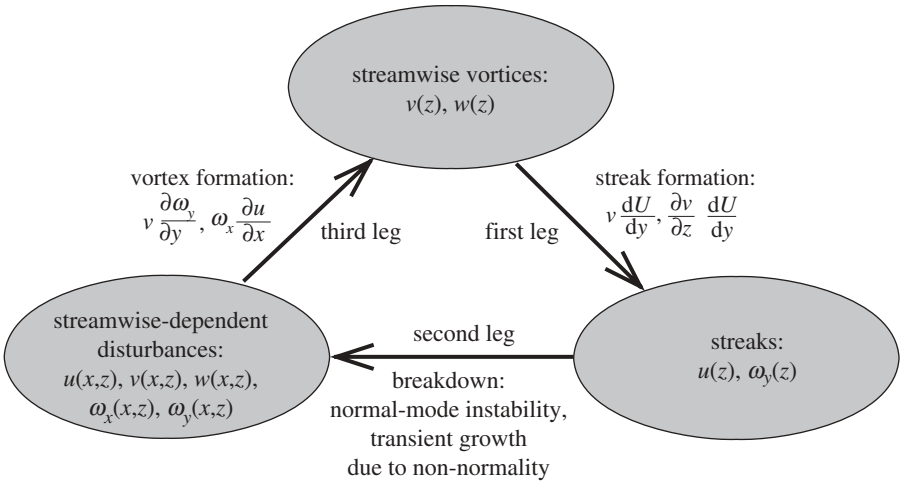

Figure 2. Schematic of a self-sustaining process of near-wall turbulence structures. Note that the y-dependence of flow variables is not shown for brevity.

transient growth) due to the non-self-adjoint nature of the linearized Navier–Stokes equations. They further illustrated that this transient-growth instability is much stronger than the normal-mode instability; the latter requires a rather strong spanwise gradient of the mean velocity, and has limited amplification. Two important points are worth mentioning, especially for the present discussion: both mechanisms are linear, and the streamwise-dependent disturbances that were necessary to form streamwise-independent vortices grow as a result of these instabilities.

The regeneration cycle described above is self-sustaining as it does not require an explicit interaction with the outer part of a boundary layer. In a numerical experiment, in which modified Navier–Stokes equations were solved in order to represent a turbulent channel flow without large-scale motions in the outer part, Jimenez & Pinelli [1] observed no discernible differences in the behaviour of the inner part (i.e. near-wall region), thus demonstrating that the inner part of boundary layers could be maintained autonomously by the self-sustaining process. This self-sustaining process of near-wall turbulence structures is a starting point of our discussion of controller design for drag reduction in TBLs. Streamwise vortices are responsible for the high skin-friction drag in TBLs, and they are maintained by the self-sustaining process. Our approach to reducing skin-friction drag in TBLs is therefore to develop a controller that can disrupt the above self-generating process.

3. Control of linear mechanisms

Two key mechanisms in the self-sustaining process described above are linear. In this section, I shall discuss a numerical experiment that will illustrate that one of these linear mechanisms indeed plays a key role in maintaining near-wall turbulence. It will also be shown that a controller designed to weaken this

linear mechanism by applying linear optimal control theory is indeed effective in reducing the skin-friction drag in fully turbulent (and hence nonlinear) boundary layers, thus validating the notion that an effective approach to achieving skin-friction drag reduction is through controlling the linear mechanisms in the self-sustaining process.

The streak generation mechanism (first leg in the regeneration cycle) is a simple advection of low-speed fluids in the wall region away from the wall by streamwise vortices. Recall that streamwise vortices consist of a wall-normal velocity that varies in the spanwise direction. This mechanism can be viewed from a slightly different perspective by considering the linearized Navier–Stokes equations in the following form:

$$\frac{\mathrm{d}}{\mathrm{d}t}\begin{bmatrix}\hat{v}\\ \hat{\omega}_y\end{bmatrix} = [\mathcal{A}]\begin{bmatrix}\hat{v}\\ \hat{\omega}_y\end{bmatrix}, \tag{3.1}$$

where

$$[\mathcal{A}] = \begin{bmatrix}L_{\mathrm{os}} & 0\\ L_{\mathrm{c}} & L_{\mathrm{sq}}\end{bmatrix}. \tag{3.2}$$

Here L_{os}, L_{sq} and L_{c} represent the Orr–Sommerfeld, Squire and linear coupling operators, respectively (see [2] for their definitions).

The linear operator $\mathcal{A}$ in equation (3.1) is non-normal (i.e. not self-adjoint), and hence its eigenmodes are non-orthogonal to each other, which allows the transient growth of disturbance energy even if all the individual eigenmodes are stable and decay asymptotically. More specifically, it has been shown that, owing to this non-normality of the linearized Navier–Stokes system, the so-called optimal disturbance can grow up to $\mathcal{O}(Re^2)$ in the transient time period, which is proportional to $\mathcal{O}(Re)$, possibly triggering nonlinear transition even below the critical Reynolds number predicted by classical linear stability theory (e.g. [15–17]). The major contribution to this non-normality comes from the linear coupling operator, L_{c}, in equation (3.2). The resulting coupling term, $(\mathrm{d}U/\mathrm{d}y)\mathrm{i}k_z\hat{v}$ in Fourier space or $(\mathrm{d}U/\mathrm{d}y)(\partial v/\partial z)$ in physical space, is a source term for wall-normal vorticity, $\hat{\omega}_y$, and this coupling between $\hat{v}$ and $\hat{\omega}_y$ is related to the streak creation mechanism in the self-sustaining process (first leg in the regeneration cycle).

In order to investigate the role of the linear coupling term in nonlinear flows, Kim & Lim [2] considered the following modified Navier–Stokes equations:

$$\frac{\mathrm{d}}{\mathrm{d}t}\begin{bmatrix}\hat{v}\\ \hat{\omega}_y\end{bmatrix} = \begin{bmatrix}L_{\mathrm{os}} & 0\\ 0 & L_{\mathrm{sq}}\end{bmatrix}\begin{bmatrix}\hat{v}\\ \hat{\omega}_y\end{bmatrix} + \begin{bmatrix}N_v\\ N_{\omega_y}\end{bmatrix}, \tag{3.3}$$

where N_v and N_{ω_y} denote the nonlinear terms in the Navier–Stokes equations. Note that the linear coupling term is absent. The system operator is still non-normal, since L_{os} itself is non-normal, but its non-normality is much reduced as the operator is now block symmetrical. Kim & Lim [2] referred this modified system to a virtual flow, which contains all the nonlinearity of turbulent flows but contains no coupling between wall-normal velocity and wall-normal vorticity. It can also be viewed as a turbulent flow with perfect control by which the coupling term was completely suppressed. Starting from an initial field obtained from a regular turbulent channel simulation, the above-modified nonlinear system

was integrated in time, and was compared with a nonlinear simulation with the coupling term. It was found that without the coupling term the near-wall structures first disappeared, and then turbulence intensities were significantly reduced (close to a laminar-like state, but this return to a laminar-like state may be due to the extremely low Reynolds number of their numerical experiment), thus demonstrating that the linear coupling term plays an essential role in maintaining turbulence in nonlinear flows.

Motivated by the above results, Lim [18] designed a controller using a linear quadratic regulator (LQR) synthesis[4], the objective of which was to minimize the linear coupling term. The control input was blowing and suction at the wall. Note that this controller could reduce the coupling term but could not completely eliminate it, in contrast to the virtual flow above, where the coupling term was artificially removed from the nonlinear calculations. Despite the fact that the controller was designed based on the linearized system in equation (3.1), the magnitude of the coupling term in the LQR-controlled flow (nonlinear) was substantially reduced, and the strength of near-wall turbulence substantially weakened, resulting in about a 20 per cent drag reduction [18].

The examples above illustrated that a linear mechanism plays an important role in TBLs. Other examples, especially in conjunction with closed-loop flow control, leading to the same conclusion have been reported in Lee *et al.* [19,20]. The work by Joshi *et al.* [21], who demonstrated that transition to turbulence (including transition due to finite-amplitude, hence nonlinear, disturbances) could be suppressed by a linear integral feedback controller, led to a flurry of research activity reporting successful applications of linear optimal control to turbulent and transitional flows. The interested reader is referred to Kim [22], and references therein, for further details.

The integration of fluid dynamics, turbulent flows in particular, and linear control theory had not been actively pursued before, in part owing to our belief that turbulent flows would be dominantly nonlinear, and in part owing to the fact that an extremely high-order system is needed to describe turbulent flows. Much progress has been made over the past decade since the pioneering work by Joshi *et al.* [21]. Kim & Bewley [3] provide an introduction to the essential ingredients of linear systems and control theory and its application to flow control. Many challenges—including, but not limited to, system identification, model reduction, processing a large amount of input–output data in real time, system nonlinearity and defining proper control objectives—lie ahead before the full potential of the control-theoretic approach can be realized. The interested reader is referred to Kim & Bewley [3] for further discussion on this promising new approach to flow control.

4. Estimation of control performance

The recognition that a linear mechanism plays a significant role in TBLs led Lim & Kim [23] to examine TBLs from a linear systems perspective. More specifically, they applied the singular-value decomposition (SVD) analysis in order to gain new insight into the mechanism by which various controllers were able to accomplish viscous drag reduction in TBLs. In this section, we give a brief overview of the

[4]An LQR controller minimizes a cost function consisting of quadratic terms of state variables.

SVD analysis, which was used to obtain an *a priori* estimation of controller performance—the interested reader is referred to Lim & Kim [23] for further details.

Equation (3.1) with control input can be written in the following state-space representation:

$$\frac{\mathrm{d}\mathbf{x}}{\mathrm{d}t} = \mathbf{A}\mathbf{x} + \mathbf{B}\mathbf{u} \tag{4.1}$$

and

$$\mathbf{u} = -\mathbf{K}\mathbf{x}, \tag{4.2}$$

where the vector $\mathbf{x}$ represents a 'state' of the system and the other vector $\mathbf{u}$ represents 'control', which is blowing and suction at the wall in the present study. Equation (4.1) represents a state equation inside the flow domain, which is being forced by the control input, $\mathbf{u}$, at the boundary of the domain. The system matrix $\mathbf{A}$ is related to the system operator $\mathcal{A}$ in equation (3.1), and the input matrix $\mathbf{B}$ depends on the particular method of control input. In linear optimal control theory, the gain matrix $\mathbf{K}$ is obtained such that a certain control objective is minimized.

By combining equations (4.1) and (4.2), the system equation is given as $\mathrm{d}\mathbf{x}/\mathrm{d}t = (\mathbf{A} - \mathbf{B}\mathbf{K})\mathbf{x}$. For uncontrolled cases, $\mathbf{K}$ is zero and the system equation simply becomes $\mathrm{d}\mathbf{x}/\mathrm{d}t = \mathbf{A}\mathbf{x}$. The traditional eigenvalue analysis, which predicts whether a linear system is stable or unstable based on the eigenvalues of the system, is inadequate in explaining transient growth of kinetic energy of certain disturbances in an otherwise stable system. Instead, transient growth can be analysed by applying the SVD analysis to the system operator, by which the amplification factor of initial disturbances can be determined.

To analyse transient energy growth through the SVD analysis, we consider the ratio of the kinetic energy of a disturbance at a given time (τ) to that at $t = 0$,

$$G(\tau) = \sup_{\mathbf{x}(\cdot,0)\neq 0} \frac{||\mathbf{x}(\tau)||^2}{||\mathbf{x}(0)||^2}, \tag{4.3}$$

where $||\mathbf{x}||^2$ represents the kinetic energy of $\mathbf{x}$. The kinetic energy can be expressed as $||\mathbf{x}(t)||^2 = \mathbf{x}^*(t)\mathbf{Q}\mathbf{x}(t)$, where the Hermitian matrix $\mathbf{Q}$ is defined in terms of an inner product in discrete space. The matrix $\mathbf{Q}$ can be further decomposed in the form $\mathbf{Q} = \mathbf{F}^*\mathbf{F}$, where $\mathbf{F}^*$ is the Hermitian conjugate of $\mathbf{F}$. The energy growth ratio can then be expressed as

$$G(\tau) = \sup_{\mathbf{x}(\cdot,0)\neq 0} ||\mathbf{F}\exp[(\mathbf{A} - \mathbf{B}\mathbf{K})\tau]\mathbf{F}^{-1}||_2^2, \tag{4.4}$$

where $||\cdot||_2$ represents the 2-norm (Euclidian norm). The 2-norm of a matrix can be easily computed from the SVD of the matrix. Typical SVD software provides a diagonal matrix $\boldsymbol{\Sigma}$ and two orthogonal matrices $\mathbf{U}$ and $\mathbf{V}$, with which any matrix can be expressed in the following form:

$$\mathbf{U}^*\mathbf{A}\mathbf{V} = \boldsymbol{\Sigma}. \tag{4.5}$$

The column vectors of $\mathbf{V}$ and $\mathbf{U}$ are referred to as right and left singular vectors, respectively. The diagonal elements of $\boldsymbol{\Sigma}$ are the singular values (σ), each of which represents the 2-norm ratio of corresponding column vectors of $\mathbf{V}$ and $\mathbf{U}$.

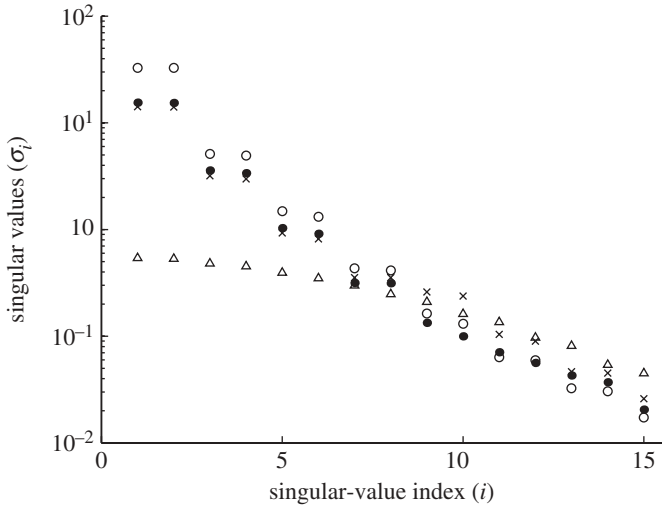

Figure 3. Singular values in a turbulent channel with different controllers: open circle, no control; filled circle, opposition control; cross, LQR control; open triangle, virtual flow.

The singular values of $\mathbf{F}\exp[(\mathbf{A}-\mathbf{BK})\tau]\mathbf{F}^{-1}$ represent the amplification of the initial kinetic energy over time τ. In naturally evolving turbulent channel flows, only a few singular values are larger than one, as shown in figure 3, implying that only a few particular disturbances can have transient growth. The largest σ represents the maximum energy growth ratio at τ, and the corresponding column vectors of $\mathbf{U}$ and $\mathbf{V}$ are the flow field at τ, and the initial flow field, respectively. In other words, the initial flow field V_1 evolves in time τ to become U_1 with the growth ratio $G(\tau)=\sigma_1$, where σ_1 is the largest singular value. Note that the singular vectors are orthogonal to each other (both $\mathbf{U}$ and $\mathbf{V}$ are orthogonal matrices), and each singular vector can be expressed in terms of a combination of the eigenvectors of the system.

The singular vector V_1 corresponding to the largest $G(\tau)$ for all wavenumber pairs is the so-called optimal disturbance. The term 'optimal' was originally chosen in the sense that this disturbance would have the largest (optimal) transient growth [16]. In a turbulent (hence nonlinear) flow environment, the evolution of this disturbance represents the most probable scenario, at least linearly, to grow and survive in the disruptive environment. In a turbulent flow environment, the given time scale, τ, plays an important role in determining the optimal disturbance. The time scale that was 'globally' optimal for the maximum energy growth was found to be relatively large ($\sim\mathcal{O}(Re)$), and Butler & Farrell [24] argued that such an optimal disturbance could not attain its potentially maximum state, as nonlinear activities constantly disrupt the linear process. They used the eddy turn-over time in the near-wall region, approximately $t^+=80$ for their τ, which resulted in an optimal disturbance similar to those observed in TBLs.

Singular values corresponding to a turbulent channel flow with various different control schemes have been examined, and the results are shown in figure 3. In addition to the channel flow with a linear optimal controller (i.e. the control

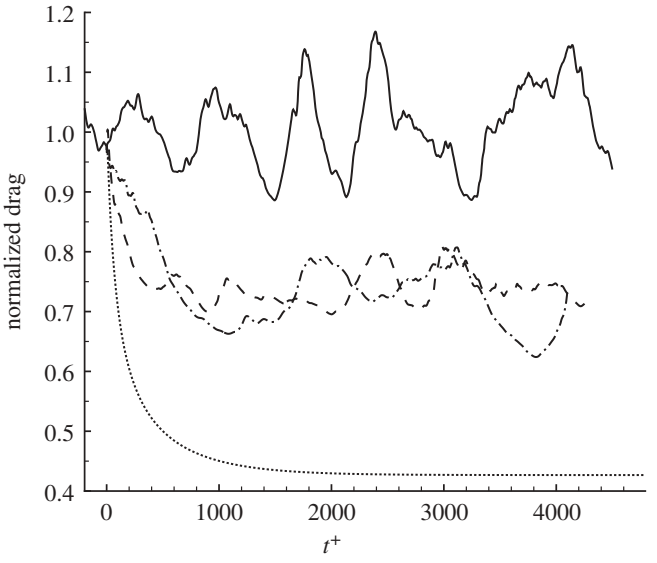

Figure 4. Mean skin-friction drag history with various control methods: solid line, no control; dashed line, opposition control ($y_d^+ \approx 15$); dashed-dotted line, LQR control; dotted line, virtual flow.

gain matrix **K** determined by an LQR synthesis), results from the opposition control[5] of Choi *et al.* [25] (see [23] for the structure of **K** corresponding to the opposition control) and those from Kim & Lim's [2] virtual flow (i.e. the operator **A** with $L_c = 0$) are also shown in figure 3. From the distribution of large singular values corresponding to different control approaches, the efficacy of each controller can be predicted, assuming that the present SVD analysis is still valid for the actual nonlinear system (see below). Note that no singular values corresponding to the virtual flow are larger than one, indicating that there would be no transient growth for any disturbance in this case.

The above SVD analysis shows how various controllers are effective in reducing the singular values associated with a linear system. Note that the reduction of singular value is related to the reduction of non-normality of the flow system, which is partially responsible for sustaining near-wall turbulence structures (which are in turn responsible for high skin-friction drag in TBLs). There is no guarantee, however, that these controllers will be equally effective in nonlinear flows. Figure 4 shows mean skin-friction drag history from numerical simulations of a turbulent channel flow (i.e. nonlinear system) with various controllers. Note that the case without the linear coupling term (virtual flow) resulted in complete laminarization, consistent with the SVD analysis. Other cases are also consistent with the SVD analysis, demonstrating that the SVD analysis is indeed a viable tool in predicting the performance of a controller in nonlinear turbulent channel

[5]Opposition control employs blowing and suction at the wall opposite to wall-normal velocity at a certain y-location in order to control near-wall streamwise vortices.

flow. It should be noted that these simulations were performed at an extremely low Reynolds number, and extending these results to much higher Reynolds number flows must be done with some care.

Lim & Kim [23] also applied the SVD analysis to opposition control with different detection planes in order to explain the observed behaviour, and the results were consistent with the reported results: that is, the largest singular value is at its minimum when the detection plane is located at $y^+ \approx 10$–15, and larger than that for the uncontrolled case with the detection plane located beyond $y^+ \approx 20$. They also showed that the efficiency of opposition control would decrease as the Reynolds number increased, consistent with the large eddy simulation (LES) results by Chang *et al.* [26], thus indirectly validating the application of the present SVD analysis, at least for opposition control, to higher Reynolds numbers.

5. Limitation of control performance

Understanding performance limitations is of great importance in designing a controller for turbulent flows, as it provides guidance as to what can be accomplished by control input. In this regard, it is worth discussing Bewley's conjecture [27] on the fundamental performance limit:

> The lowest sustainable drag of an incompressible constant mass-flux channel flow, when controlled via a distribution of zero-net mass-flux blowing/suction over the no-slip channel walls, is exactly that of the laminar flow.

Bewley's conjecture can be elucidated by a useful expression for skin-friction drag in fully developed channel flows [27,28]:

$$D = \frac{1}{2}\left(\left.\frac{\mathrm{d}U}{\mathrm{d}y}\right|_{-1} - \left.\frac{\mathrm{d}U}{\mathrm{d}y}\right|_{1}\right) = 2 + \frac{3}{2}Re\int_{-1}^{1}\overline{u'v'}\,y\,\mathrm{d}y. \tag{5.1}$$

Here, all quantities are normalized by the centreline velocity (U_c) and the channel half height (h), U denotes the mean velocity, Re the Reynolds number based on the laminar centreline velocity, and $\overline{u'v'}$ is the Reynolds shear stress. Note that equation (5.1) is valid for all channel flows with the same mass flux as the base laminar flow (4/3 with the present normalization). The first term on the right-hand side of equation (5.1) represents the mean wall-shear rate of laminar flow ($U = 1 - y^2$), and therefore equation (5.1) shows that skin-friction drag in a channel flow consists of the laminar drag plus the y-weighted integral of $\overline{u'v'}$. From the viewpoint of equation (5.1), Bewley's conjecture is equivalent to saying that the y-weighted integral of $\overline{u'v'}$, with and without control input, is always positive in channel flows. For a regular channel flow without control, this is the case, since the Reynolds shear stress in the lower half of the channel ($-1 < y < 0$) is negative, while the opposite is true in the upper half of the channel ($0 < y < 1$). As such, the skin-friction drag in transitional and turbulent channel flows is higher than that of the corresponding laminar flow with the same mass flux. Bewley & Aamo [27] reported that they could not sustain the Reynolds shear stress, which could yield a drag below the laminar value. Based on

their numerical experiments, they provided phenomenological justification of Bewley's conjecture, but they left the proof of the conjecture as an open problem.

Bewley's conjecture turned out to be incorrect, as demonstrated by Min *et al.* [29], who discovered serendipitously that sustainable sub-laminar drag could be achieved when a channel flow was subjected to periodic open-loop blowing and suction at the wall in the form of an upstream travelling wave. It was shown that certain upstream travelling waves induce the Reynolds shear stress in such a way that it makes a negative contribution to the total viscous drag. With a large amplitude of open-loop control in the form of an upstream travelling wave, they were able to reduce the viscous drag in turbulent channel to a sub-laminar value. However, they observed that the efficiency of their open-loop control was better with a smaller amplitude of control input, which resulted in larger than laminar drag (but still lower than the uncontrolled turbulent drag). Further discussions on this periodic open-loop control and a Floquet stability analysis of the periodic control can be found in Lee *et al.* [30].

Luchini [31] later argued that Min *et al.*'s [29] periodic blowing and suction at the wall induced a steady streaming (or Rayleigh streaming) phenomenon, which led to additional mean flux in the streamwise direction. As such, Luchini asserted that Min *et al.*'s open-loop control did not reduce the drag directly but provided additional pumping (or thrust), thus reducing the required pressure gradient for a given mass flux. However, it was clear in Min *et al.*'s simulation of controlled turbulent flows that, in addition to more pumping due to the steady streaming effect, near-wall turbulence structures were reduced (or completely disappeared with stronger blowing and suction), thus directly affecting those near-wall turbulence structures responsible for high skin friction. It is apparent that travelling-wave-induced Reynolds shear stress in TBLs played two distinctive roles: that is, additional pumping due to the Rayleigh streaming, and reduction of drag by modifying near-wall turbulence structures. Hoepffner & Fukagata [32] reported further analysis on the effects of blowing and suction at the wall as well as the effects of travelling waves of wall deformation (peristalsis). They proposed a power-plane diagram with which the true efficiency of control performance can be compared.

Bewley [33] extended his earlier analysis of channel flow subject to blowing and suction at the wall and modified the above-mentioned conjecture. He showed that energetically (that is, considering the total power, accounting for both the power saved and the additional power for control input, for a given mass flux) the best one can do is to maintain a laminar flow. This result is consistent with Min *et al.*'s [29] observation mentioned above and with the analysis of Fukagata *et al.* [34], who showed that the parabolic profile in the channel has the least viscous dissipation. All of these results point to a fundamental performance limitation for controllers designed for viscous drag reduction: maintaining the laminar drag is the most optimal energetically. Thus, although one can achieve a flow with sub-laminar drag with certain control input, it would not be the most optimal from the energetic point of view. The ultimate goal of control input for the purpose of drag reduction is then to achieve a laminar flow. It should be noted that both Bewley's and Fukagata *et al.*'s proofs are for channel flows, although it is probable that a similar proof (that is, the best one can do for spatially developing boundary layers is to maintain a laminar boundary layer) is possible for boundary layers.

6. Beyond simple flows

All discussions in this paper have been limited to simple canonical wall-bounded shear flows (i.e. turbulent channel flows or boundary layers), for which we assume that the linearized system operator, **A** in equation (4.2), is readily available, or reduced-order models can be constructed easily if the size of **A** is too large to be handled directly [3]. It is not straightforward, however, to extend this linear systems approach to control problems involving a complex flow. For complex flows, explicit representations of system matrices (e.g. **A** and **B** in equation (4.2)) are generally not readily available or they become too large even if they can be directly computed. Standard Fourier decomposition is inapplicable owing to flow inhomogeneity and geometry, and the resulting system matrices could be too large to handle in practice. Also, the control goals may be quite different from viscous drag reduction of boundary layers.

Huang & Kim [35] explored an approach by which systems-theory-based flow control could be extended to more complex flows. Instead of deriving the system model directly from linearized governing equations of the fluid flow, they employed a system identification approach to generate approximate system matrices using only the input–output data sequences. Using these approximate linear system models, they obtained a reduced-order model by applying a balanced-order model reduction technique. Based on the reduced-order model, feedback control laws were then constructed and applied to the control of a separated boundary layer. It was shown that the separation bubble size could be reduced by the closed-loop control, although they also reported difficulty in formulating a proper control objective (i.e. expressing reduction of separation bubble in terms of state variables) to be optimized. While much more work is needed to improve the modelling accuracy and control performance, their work represented a promising step towards extending the linear systems approach to complex flows.

7. Summary and concluding remarks

The near-wall turbulence structures responsible for increased skin-friction drag in TBLs are regenerated autonomously in the wall region by a self-sustaining process. Key elements in the self-sustaining process are linear, and are subject to linear analysis. It is shown that boundary layers can be analysed from a linear system perspective. The SVD analysis can provide useful information regarding the controller's capability of attenuating the transient growth of disturbances in TBLs. The trends observed from the SVD analysis were similar to those observed in direct numerical simulation (DNS) or LES of drag-reduced turbulent flows, illustrating that the linear system model can describe an important part of the near-wall dynamics and that it can be used as a guideline for various control designs for drag reduction. It could be used, for example, in optimizing control parameters without actually performing expensive nonlinear computations. Other issues, such as the effects of using the evolving mean flow as control applied to a nonlinear flow system (also known as gain scheduling), and high Reynolds number limitations, can also be addressed through the SVD analysis. Although the entire discussion on the performance of various control approaches is based on numerical experiments (and have yet to be verified in laboratory experiments), they have

shown great promise and present a new approach to flow control. Considering the fundamental performance limitation of the boundary-layer control, the ultimate goal for control of TBLs for the purpose of drag reduction is to relaminarize turbulent boundary layers. One can achieve a flow with lower-than-laminar drag, but it would not be optimal energetically.

All control approaches discussed in the present paper were aimed at controlling near-wall turbulence structures, streamwise vortices in particular, under the assumption that they were primarily responsible for high skin-friction drag in TBLs. This assumption was based on our observations of TBLs, both experimentally and numerically, at relatively low Reynolds numbers. On the other hand, some researchers have raised a concern that TBLs may behave completely differently at high Reynolds numbers. J. C. R. Hunt (2010, personal communication), for example, argued that, while a 'bottom-up' process (i.e. the inner part of the boundary layer drives the outer part) is dominant at low Reynolds numbers, a 'top-down' process (i.e. the outer part drives the inner part) may play a dominant role at high Reynolds numbers. If this scenario turns out to be true, near-wall turbulence structures, even if they exist in TBLs at high Reynolds numbers, may not play the dominant role, and hence controlling near-wall turbulence structures would not be as effective in reducing skin-friction drag at high Reynolds numbers. One counter-example illustrating that controlling near-wall turbulence structures would still be effective at high Reynolds numbers is a flight-test experiment carried out by Boeing [36], in which noticeable drag reduction was observed on a riblet surface at a relatively high Reynolds number. Since a riblet surface is known to reduce drag through interactions with near-wall turbulence structures [37], this is indirect evidence that near-wall turbulence structures do exist and still play an important role in TBLs at high Reynolds numbers. Further work is necessary in order to address the question regarding the 'bottom-up' versus 'top-down' process and the role of near-wall turbulence structures in TBLs at high Reynolds numbers.

Much of the discussion in this paper is based on the linearized Navier–Stokes equations, the use of which can be justified by the fact that a linear mechanism plays an essential role in the self-sustaining process of near-wall turbulence. It should be noted, however, that linearized Navier–Stokes equations are not sufficient to describe many features of TBLs, including the self-sustaining process of near-wall turbulence, in which a nonlinear mechanism also plays an essential role. It is worth pointing out that identifying and controlling a linear mechanism in nonlinear flows is not equivalent to trying to describe nonlinear flows with a linear model. This limitation notwithstanding, it is shown here that much can be learned from a proper linear analysis of nonlinear flows, especially for the wall-bounded turbulent shear flows where a linear mechanism plays an important, if not dominant, role. In this regard, and to some extent paradoxically, wall-bounded turbulent shear flows are more amenable to a theoretical analysis than, say, homogeneous isotropic turbulent flows, where no dominant linear mechanism is present.

Many current and former colleagues at UCLA, NASA Ames Research Center and Stanford University have contributed to the results reviewed in this paper, and I thank them all. The financial support I have received from the Air Force Office of Scientific Research and the Office of Naval Research during the course of this work is also gratefully acknowledged. The computer time has been provided by NSF through the NRAC and TRAC programs.

References

1 Jimenez, J. & Pinelli, A. 1999 The autonomous cycle of near-wall turbulence. *J. Fluid Mech.* **389**, 335–359. (doi:10.1017/S0022112099005066)

2 Kim, J. & Lim, J. 2000 A linear process in wall-bounded turbulent shear flows. *Phys. Fluids* **12**, 1885–1888. (doi:10.1063/1.870437)

3 Kim, J. & Bewley, T. R. 2007 A linear systems approach to flow control. *Annu. Rev. Fluid Mech.* **39**, 383–417. (doi:10.1146/annurev.fluid.39.050905.110153)

4 Kim, J., Moin, P. & Moser, R. D. 1987 Turbulence statistics in fully developed channel flow at low Reynolds number. *J. Fluid Mech.* **177**, 133–166. (doi:10.1017/S0022112087000892)

5 Dubief, Y., White, C. M., Terrapon, V. E., Shaqfeh, E. S. G., Moin, P. & Lele, S. K. 2004 On the coherent drag-reducing and turbulence-enhancing behaviour of polymers in wall flows. *J. Fluid Mech.* **514**, 271–280. (doi:10.1017/S0022112004000291)

6 Min, T., Yoo, J. Y., Choi, H. & Joseph, D. D. 2003 Drag reduction by polymer additives in a turbulent channel flow. *J. Fluid Mech.* **486**, 213–238. (doi:10.1017/S0022112003004610)

7 Ferrante, A. & Elghobashi, S. 2004 On the physical mechanisms of drag reduction in a spatially developing turbulent boundary layer laden with microbubbles. *J. Fluid Mech.* **503**, 345–355. (doi:10.1017/S0022112004007943)

8 Min, T. & Kim, J. 2004 Effects of hydrophobic surface on skin-friction drag. *Phys. Fluids* **16**, L55–L58. (doi:10.1063/1.1755723)

9 Hamilton, J. M., Kim, J. & Waleffe, F. 1995 Regeneration mechanisms of near-wall turbulence structures. *J. Fluid Mech.* **287**, 317–348. (doi:10.1017/S0022112095000978)

10 Schoppa, W. & Hussain, F. 2002 Coherent structure generation in near-wall turbulence. *J. Fluid Mech.* **453**, 57–108. (doi:10.1017/S002211200100667X)

11 Waleffe, F. 1997 On a self-sustaining process in shear flows. *Phys. Fluids* **9**, 883–900. (doi:10.1063/1.869185)

12 Waleffe, F. & Kim, J. 1997 How streamwise rolls and streaks self-sustain in a shear flow. In *Self-sustaining mechanisms of wall turbulence* (ed. R. Panton). Southampton, UK: Computational Mechanics Publications.

13 Kim, J. 1987 Evolution of a vortical structure associated with the bursting event in a channel flow. In *Turbulent shear flows 5* (eds F. Durst, B. Launder, J. Lumley, F. Schmidt & J. Whitelaw). Berlin, Germany: Springer.

14 Zhou, J., Adrian, R. J., Balachandar, S. & Kendall, T. M. 1999 Mechanisms for generating coherent packets of hairpin vortices in channel flow. *J. Fluid Mech.* **387**, 353–396. (doi:10.1017/S002211209900467X)

15 Bamieh, B. & Dahleh, M. 2001 Energy amplification in channel flows with stochastic excitation. *Phys. Fluids* **13**, 3258–3269. (doi:10.1063/1.1398044)

16 Butler, K. M. & Farrell, B. F. 1992 Three-dimensional optimal perturbations in viscous shear flow. *Phys. Fluids A* **4**, 1637–1650. (doi:10.1063/1.858386)

17 Reddy, S. C. & Henningson, D. S. 1993 Energy growth in viscous channel flows. *J. Fluid Mech.* **252**, 209–238. (doi:10.1017/S0022112093003738)

18 Lim, J. 2003 A linear control in turbulent boundary layers. PhD. dissertation, University of California, Los Angeles.

19 Lee, C., Kim, J., Babcock, D. & Goodman, R. 1997 Application of neural networks to turbulence control for drag reduction. *Phys. Fluids* **9**, 1740–1747. (doi:10.1063/1.869290)

20 Lee, C., Kim, J. & Choi, H. 1998 Suboptimal control of turbulent channel flow for drag reduction. *J. Fluid Mech.* **358**, 245–258. (doi:10.1017/S002211209700815X)

21 Joshi, S. S., Speyer, J. L. & Kim, J. 1997 A systems theory approach to the feedback stabilization of infinitesimal and finite-amplitude disturbances in plane Poiseuille flow. *J. Fluid Mech.* **332**, 157–184. (doi:10.1017/S0022112096003746)

22 Kim, J. 2003 Control of turbulent boundary layers. *Phys. Fluids* **15**, 1093–1105. (doi:10.1063/1.1564095)

23 Lim, J. & Kim, J. 2004 A singular value analysis of boundary layer control. *Phys. Fluids* **16**, 1980–1987. (doi:10.1063/1.1710522)

24 Butler, K. M. & Farrell, B. F. 1993 Optimal perturbations and streak spacing in wall-bounded turbulent shear flow. *Phys. Fluids A* **5**, 774–777. (doi:10.1063/1.858663)
25 Choi, H., Moin, P. & Kim, J. 1994 Active turbulence control for drag reduction in wall-bounded flows. *J. Fluid Mech.* **262**, 75–110. (doi:10.1017/S0022112094000431)
26 Chang, Y., Collis, S. S. & Ramakrishnan, S. 2002 Viscous effects in control of near-wall turbulence. *Phys. Fluids* **14**, 4069–4080. (doi:10.1063/1.1509751)
27 Bewley, T. R. & Aamo, O. M. 2004 A 'win–win' mechanism for low-drag transients in controlled two-dimensional channel flow and its implications for sustained drag reduction. *J. Fluid Mech.* **499**, 183–196. (doi:10.1017/S0022112003006852)
28 Fukagata, K., Iwamoto, K. & Kasagi, N. 2002 Contribution of Reynolds shear stress distribution to the skin friction in wall-bounded flows. *Phys. Fluids* **14**, L73–L76. (doi:10.1063/1.1516779)
29 Min, T., Kang, S. M., Speyer, J. L. & Kim, J. 2006 Sustained sub-laminar drag in a fully developed channel flow. *J. Fluid Mech.* **558**, 309–318. (doi:10.1017/S0022112006000206)
30 Lee, C., Min, T. & Kim, J. 2008 Stability of channel flow subject to wall blowing and suction in the form of a traveling wave. *Phys. Fluids* **20**, 10153. (doi:10.1063/1.3006057)
31 Luchini, P. 2006 Acoustic streaming and lower-than-laminar drag in controlled channel flow. In *Progress in industrial mathematics at ECMI*. Mathematics in industry, vol. 12, pp. 169–177. Berlin, Germany: Springer.
32 Hoepffner, J. & Fukagata, K. 2009 Pumping or drag reduction? *J. Fluid Mech.* **635**, 171–187. (doi:10.1017/S0022112009007629)
33 Bewley, T. R. 2009 A fundamental limit on the balance of power in a transpiration-controlled channel flow. *J. Fluid Mech.* **632**, 443–446. (doi:10.1017/S0022112008004886)
34 Fukagata, K., Sugiyama, K. & Kasagi, N. 2009 On the lower bound of net driving power in controlled duct flows. *Physica D* **238**, 1082–1086. (doi:10.1016/j.physd.2009.03.008)
35 Huang, S.-C. & Kim, J. 2008 Control and system identification of a separated flow. *Phys. Fluids* **20**, 101509. (doi:10.1063/1.3005860)
36 McLean, J. D., George-Falvy, D. N. & Sullivan, P. P. 1987 Flight-test of turbulent skin friction reduction by riblets. In *Proc. Int. Conf. on Turbulent Drag Reduction by Passive Means*, Section 16, pp. 1–17. London, UK: Royal Aeronautical Society.
37 Choi, H., Moin, P. & Kim, J. 1993 Direct numerical simulation of turbulent flow over riblets. *J. Fluid Mech.* **255**, 503–539. (doi:10.1017/S0022112093002575)